Towards harmonization of image velocimetry techniques for river surface velocity observations

Matthew. T. Perks[1], Silvano Fortunato Dal Sasso[2], Alexandre Hauet[3], Jérôme Le Coz[4], Sophie Pearce[5], Salvador Peña-Haro[6], Flavia Tauro[7], Salvatore Grimaldi[7, 8], Borbála Hortobágyi[1], Magali Jodeau[9,10], Ian Maddock[5], Lionel Pénard[4], and Salvatore Manfreda[2]

[1]School of Geography Politics and Sociology, Newcastle University, Newcastle upon Tyne, United Kingdom
[2]Department of European and Mediterranean Cultures: Architecture, Environment and Cultural Heritage (DiCEM), University of Basilicata, 75100 Matera, Italy
[3]Electricité de France, DTG, Grenoble, France
[4]Irstea, UR RiverLy, River Hydraulics, Villeurbanne, France
[5]School of Science and the Environment, University of Worcester, Worcester, UK.
[6]Photrack AG: Flow Measurements, Ankerstrasse 16a, 8004 Zürich, Switzerland
[7]Department for Innovation in Biological, Agro-food and Forest Systems, University of Tuscia, Viterbo, Italy
[8]Department of Mechanical and Aerospace Engineering, Tandon School of Engineering, New York University, Brooklyn, NY, United States.
[9]Electricité de France, R&D, Chatou, France
[10]LHSV, Chatou, France

Correspondence: Matthew T. Perks (matthew.perks@ncl.ac.uk)

Abstract. Since the turn of the 21st Century, image based velocimetry techniques have become an increasingly popular approach for determining open-channel flow in a range of hydrological settings across Europe, and beyond. Simultaneously, a range of large-scale image velocimetry algorithms have been developed, equipped with differing image pre-processing, and analytical capabilities. Yet in operational hydrometry, these techniques are utilised by few competent authorities. Therefore,

5 imagery collected for image velocimetry analysis, along with validation data is required both to enable inter-comparisons between these differing approaches and to test their overall efficacy. Through benchmarking exercises, it will be possible to assess which approaches are best suited for a range of fluvial settings, and to focus future software developments. Here we collate, and describe datasets acquired from six countries across Europe and Asia, consisting of videos that have been subjected to a range of pre-processing, and image velocimetry analysis (Perks et al., 2019, https://doi.org/10.4121/uuid:

10 34764be1-31f9-4626-8b11-705b4f66b95a). Validation data is available for 12 of the 13 case studies presented enabling these data to be used for validation and accuracy assessment.

1 Introduction

When designing hydrological monitoring networks, or acquiring opportunistic measurements for determining open-channel flow, the optimum choice of apparatus is likely to be a compromise between the data requirements, resource availability,

15 and the hydro-geomorphic characteristics of the site (Mishra and Coulibaly, 2009). Generally, hydro-geomorphic factors will include: channel width and depth, the range of flow velocities, presence of secondary circulation, and cross-section stability.

Each field measurement technique will have a designed range of optimum operating conditions, under which, robust flow measurements should be expected (e.g. ISO 24578:2012). However, under conditions beyond their designed operating range, greater levels of uncertainty will ensue. This may therefore preclude certain approaches for deployment under very shallow, or flood flow conditions for example. Logistical and practical constraints may also limit the deployment of apparatus. For example, techniques that require the device to be in contact with the water during operation may not be feasible for health and safety reasons during periods of high-flow, or due to staff availability (Harpold et al., 2006). As a result of some of these challenges, the potential for implementing alternative, non-contact approaches has been recently explored. Within this field of research, image velocimetry has emerged as an exciting new approach for determining a key hydrological characteristic, namely flow velocity.

Image velocimetry involves the application of cross-correlation, or computer vision techniques to a series of consecutive images (or extracted video frames) to generate vectors of water velocities across a field-of-view. It was originally developed for use in highly controlled laboratory settings. However, since its original conception, its application has expanded from use in the laboratory (e.g., Dudderar and Simpkins, 1977; Adrian, 1984; Pickering and Halliwell, 1984), to include a wide variety of experimental conditions. Most notably it has been deployed outside of the controlled environment of the laboratory and into the domain of the field scientist (e.g., Fujita et al., 1998). It is now applied in complex environments including situations where lighting is not controlled, the camera platform may be mobile (e.g. on unmanned aerial systems (UAS)), images may be acquired oblique to the direction of flow, and at an angle that changes over time (e.g. Detert and Weitbrecht, 2015; Tauro et al., 2016b; Perks et al., 2016).

This technique is also becoming increasingly popular with the wider hydrological community (Tauro et al., 2018a), and this has been aided by two key factors. The first of which is the development of platforms and hardware that enable high-definition images and videos to be captured precisely, stored, and transferred to locations where image processing can occur. Secondly, many researchers utilizing image velocimetry techniques have chosen to develop their own specific processing capabilities, leading to the development of a range of both open-source and proprietary software for image pre-processing, and velocimetry analysis (Table A1). Whilst this has led to a breadth of options for researchers conducting image velocimetry analysis, inter-comparisons of their efficacy under a range of environmental settings, and flow regimes is currently lacking. Therefore, there is an urgent need to comprehensively understand and appreciate limitations of the differing image velocimetry approaches that are available to the scientific community.

Here, we present a range of datasets that have been compiled from across six countries in order to facilitate these inter-comparison studies (Figure 1, Perks et al. (2019)). These data have been independently produced for the primarily purposes of: (i) enhancing our understanding of open-channel flows in diverse flow regimes; and (ii) testing specific image velocime-try techniques. These datasets have been acquired across a range of hydro-geomorphic settings, using a diverse range of cameras, encoding software, controller units, and with river velocity measurements generated as a result of differing image pre-processing and image processing software.
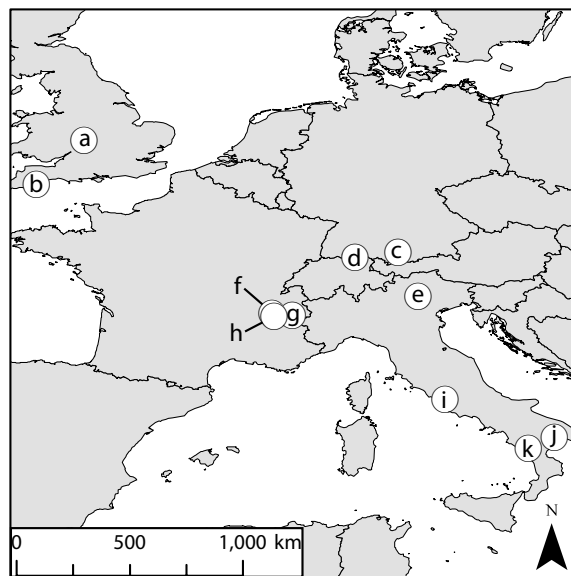
Figure 1. Geographical locations of the monitoring sites from which data presented: (a) River Arrow, UK; (b) River Dart, UK; (c) River Thalhofen, Germany; (d) Murg River, Switzerland; (e) River Brenta, Italy; (f) La Morge, France; (g) St-Julien torrent, France; (h) River La Vence, France; (i) River Tiber, Italy; (j) River Bradano, Italy; (k) River Noce, Italy. Not shown: River Karehalla, India. Map spatial reference: ETRS (1989).

2 Experimental Design

Given the range of image velocimetry techniques that have been developed in recent years, benchmarking datasets covering a range of hydro-geomorphic conditions and acquisition platforms are required in order to test the accuracy and precision of each algorithm for the determination of 2-dimensional surface velocities. The examples that we describe in this section have

5   been acquired by a range of platforms including UAS, fixed and hand-held cameras. The geographical characteristics of the sites are also widely varied. Catchment areas span $20–17\,460\,\mathrm{km}^2$, captured channel widths range from 5–28 m, minimum flow depth is $0.22\,\mathrm{m}$, with a maximum of over $7\,\mathrm{m}$, and mean flow velocities range from 0.3 to over $6\,\mathrm{m\,s}^{-1}$. Where possible, validation data generated by established and widely accepted approaches (e.g. electromagnetic current meter, and acoustic Doppler current profiler (ADCP)) have been collected simultaneously, or at the same river stage as images are acquired. The

10   details pertaining to the hydrological conditions of deployment, configuration of the camera setup, pre-processing of imagery, and where relevant, details of published results from these datasets are presented in the following sections and summarised in Table A2.

2.1 River Arrow, UK

On 1ˢᵗ November 2017, a field experiment was undertaken on the River Arrow in Warwickshire (UK), to ascertain the accuracy of two differing image velocimetry approaches. The location of this experiment was in the mid-reaches of the catchment with a contributing area of 319km². This is a stable, meandering section of the river with an approximate width of $5\,\mathrm{m}$. During the experiment, mean depth and velocity were $0.22\,\mathrm{m}$ and $0.42\,\mathrm{m\,s^{-1}}$ respectively and water turbidity was minimal with the gravel bed being distinctly visible in the footage. The two deployments differed as both fixed and mobile imaging systems were used. Footage acquired from these two systems was captured concurrently, permitting direct comparisons to be made between the two. The mobile imaging system consisted of a DJI Phantom 4 Pro UAS equipped with a 1" camera CMOS sensor. This was used to collect nadiral footage with the camera's y-axis orthogonal to the direction of flow. Video was collected by the UAS for $4\,\mathrm{min}\,18\,\mathrm{s}$ whilst hovering in an approximately stationary position at an elevation of approximately $20\,\mathrm{m}$ over the field of interest (Figure 2a). Footage was recorded at a pixel resolution of 1920×1080, and frame rate of $30\,\mathrm{Hz}$. The second approach consisted of a GoPro Hero 4 mounted at an oblique angle on a stationary telescopic pole at a height of approximately $2\,\mathrm{m}$ above the water surface. Video footage was simultaneously collected for $5\,\mathrm{min}\,37\,\mathrm{s}$ at a pixel resolution of 1920×1080, and frame rate of $30\,\mathrm{Hz}$. During this period of recording, sequences consisting of both unseeded flow, and artificially seeded flow are visible. For the seeded element, cornstarch ecofoam chips were added to the water surface immediately upstream of the area of interest. These tracers are clearly visible in the footage and are distributed evenly in the cross-section. Seeding was carried out to enhance the availability of traceable features in the low-flow conditions. From the recordings, four datasets each consisting of 99 consecutive images (sampled at a frame rate of $5\,\mathrm{Hz}$, and converted to grayscale intensity) were extracted from both the UAS and GoPro footage under both seeded and unseeded conditions. In order to enable the conversion of pixel units to metric units a total of ten ground control points (GCPs), which were visible throughout the duration of the video, were distributed across both banks (Figure 2a). These GCPs were surveyed and their positions utilised for image orthorectification using Fudaa-LSPIV (Table A1). Subsequently, the orthorectified images have a scaling of $0.0174\,\mathrm{m\,px^{-1}}$ (Figure 2b). Validation data was obtained for five cross-sections, spaced approximately 1.5–2 m apart through the use of a Valeport electromagnetic current meter. This velocity data was obtained just below the water surface.

2.2 River Dart, UK

In the UK, a dense network of hydrometric monitoring stations is in place for both water resources and flood prediction purposes. However, under the most challenging conditions, current operational approaches for monitoring river flow may be sub-optimal. The first of a series of image-based monitoring solutions was installed on the River Dart in collaboration with the Environment Agency. This is a rapidly responding $248\,\mathrm{km^2}$ catchment draining the uplands of Dartmoor, with a channel width of $25\,\mathrm{m}$ under normal flow conditions. Here, a Hikvision DS-2CD2T42WD-I8 $6\,\mathrm{mm}$ IP camera was mounted at an oblique angle ($77°$ from nadir), and connected to a Raspberry Pi 3 Model B. This system was configured to record and transmit videos at a resolution of $1920 \times 1080\mathrm{px}$ and a frame rate of $19\,\mathrm{Hz}$ to online servers (AWS S3). The system was commissioned in March 2018 and has since been collecting and transmitting $10\,\mathrm{s}$ videos at $15\,\mathrm{min}$ intervals. No artificial tracers are introduced
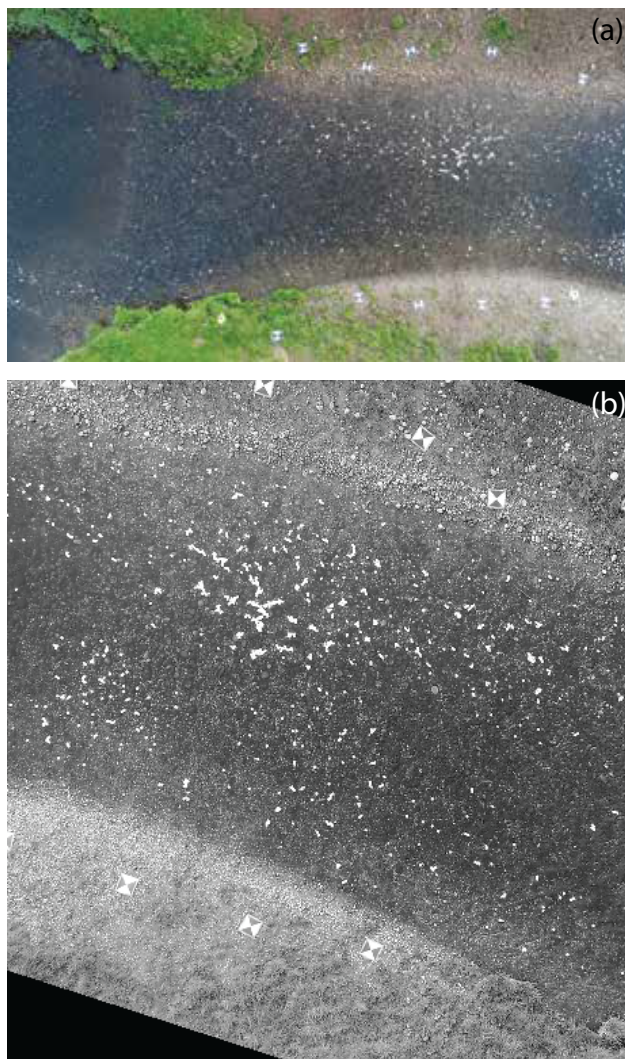
Figure 2. (a) Footage acquired by the Phantom 4 UAS over the River Arrow, and (b) following orthorectification and grayscale conversion. The Ecofoam chips and ground control points are clearly visible in both images.

to the fluvial environment to aid tracking, rather the presence of naturally occurring features are used in the analysis of surface velocities. Following collection, images underwent correction for lens distortion, and have been orthorectified using KLT-IV (Table A1). This results in images where each pixel has a spatial scale of $0.02\,\mathrm{m}$. Here we present five sequences of orthorectified images collected across a range of flows spanning approximately three orders of magnitude (10^0 - $10^2\,\mathrm{m^3\,s^{-1}}$) at the original frame rate. To supplement this footage, validation data is available in the form of acoustic Doppler current profiler transects conducted at the same river stage as the video footage was collected ($\pm\,0.01\,\mathrm{m}$).

2.3 River Thalhofen, Germany

On 27th July 2017, a Vivotek IB836BA-HT network surveillance camera was utilised to capture footage for image velocimetry analysis on the River Thalhofen in Germany. At the time of deployment, the river width was approximately $28\,\mathrm{m}$, the river stage was $1.45\,\mathrm{m}$, and ADCP derived discharge was $52.515\,\mathrm{m^3\,s^{-1}}$. The camera was fixed in location with the camera lens at an approximate angle of $25°$ from nadir and the image y-axis approximately $5°$ from being perpendicular to the direction of flow. Images were collected for a duration of $2\,\mathrm{s}$ at a resolution of $1280{\times}800\mathrm{px}$ and frame rate of $30\,\mathrm{Hz}$. Despite the presence of highly turbid water, which can diminish contrast across the water surface, the presence of highly visible turbulent structures advecting downstream offer the potential for the extraction of surface velocity information from these images. Image pre-processing consisted of orthorectification (using Photrack software), and color conversion to gray-scale. 56 consecutive images which have been subjected to these processing steps are presented here at their original frame rate of $30\,\mathrm{Hz}$. The pixel dimensions of the processed imagery are $0.01\,\mathrm{m}$ in the x and y-axis. Validation data was acquired by means of a Teledyne RiverPro ADCP.

2.4 Murg River, Switzerland

On the 4th April 2016, aerial surveys were undertaken in order to acquire imagery for determining the bathymetry, surface velocity, and to subsequently derive the flow discharge of the Murg River, Switzerland (Detert et al., 2017). The experiment took place in the middle reaches of the catchment, with a contributing area of $212\,\mathrm{km^2}$. The experimental reach was a stable, straight section totalling $75\,\mathrm{m}$ in length, along which, the water depth was approximately $0.35\,\mathrm{m}$ and channel width was $12\,\mathrm{m}$. For the aerial survey a DJI Phantom FC40 was deployed at a stable altitude of $30\,\mathrm{m}$ to track the movement of artificial tracers throughout the reach. The UAS was equipped with a GoPro Hero3+ black edition 4K camera, capable of capturing a large spatial footprint whilst deployed at a relatively low altitude. However, this also generates a considerable barrel distortion effect which must be overcome during image processing. This system was used to collect nadiral footage with the camera's y-axis perpendicular to the flow direction. Video footage was acquired for a period of $2\,\mathrm{min}\,11\,\mathrm{s}$ at a pixel resolution of $4096{\times}2160$ and a frame rate of $12\,\mathrm{Hz}$. During image acquisition, the water was clear, with the channel bed visible in places. These conditions resulted in a lack of naturally occurring features visible on the water surface that could be used to determine surface velocity. Therefore, throughout the duration of the experiment, spruce wood chips were applied to the water surface from a bridge at the upper extent of the monitored reach. This artificial seeding produced a dense, vivid, and homogeneously distributed pattern of features, the displacement rate of which is considered to equate to the surface velocity. From the video

recordings, 1000 images were orthorectified using Photoscan (Agisoft). This was achieved through the input of geographical coordinates relating to 14 GCPs that were visible at varying times throughout image sequence. This approach is discussed further in Detert et al. (2017). The subsequent orthorectified images are presented at a time-step of $0.083\,$s and the raster pixel scale was consistently set at 64px m^{-1}, equivalent to pixel dimensions of $0.0156\,$m in the x-axis and y-axis. Meta-data

5 describing the scale of the image per pixel, as well as the [x,y] coordinate of the upper left pixel of each image are provided in the corresponding .jgw file. Validation data was acquired through the deployment of a Teledyne RDI StreamPro ADCP across a single transect in the upper reaches of the studied site.

2.5 River Brenta, Italy

Two distinct experimental approaches have been adopted to generate datasets that describe flows in the $252\,$km^2 catchment of

10 the River Brenta. The first involved the temporary installation of a GoPro Hero 4 Black Edition camera attached to a telescopic apparatus on the downstream side of a bridge (Tauro et al., 2014). During this deployment, river flow was low with a lack of naturally visible tracers on the water's surface. To compensate for this, wood-chips were manually added to the river upstream of the monitoring site resulting in continuous, and relatively homogeneous coverage for the $20\,$seconds duration of the image sequences. The camera's field of view was $9.5{\times}5.3\,$m^2 and it was configured to collect $1920{\times}1080$ HD videos at a frame rate of

15 $50\,$Hz. Distortion of the images as a result of the fish-eye lens was removed using the open-source software *GoPro Studio*. No subsequent orthorectification of the images was required due to the camera apparatus being installed perpendicular to the water surface. The pixel dimensions of the processed imagery were $0.005\,$m in the x-axis and y-axis. This could be established either through the projection of two lasers at a fixed and known distance apart to the surface of the river or through identification of a fixed and known object in the field of view. In terms of pre-processing of the imagery, an area of $552{\times}375$ pixels in the bottom

20 right corner of the images was masked with a black patch. This was to eliminate noise generated by mobile vegetation within the frame. Original RGB images were converted to gray-scale intensity by eliminating hue and saturation information and retaining the luminance. To emphasize lighter particles against a dark background, images were gamma corrected to darken mid-tones. A total of twelve separate image sequences lasting twenty seconds, subsampled at $25\,$Hz, and consisting of 500 frames each are presented here.

25 The second experimental approach involved the temporary deployment of a FLIR Systems AB ThermaCAM SC500. This was suspended from a mobile supporting structure on the downstream side of a bridge at approximately $7\,$m above the water surface (Tauro and Grimaldi, 2017). As opposed to capturing images in the usual red, green, and blue bands, this camera is sensitive to thermal infrared radiation, generating a monochrome image with values proportionate to the thermal properties of the objects within the field of view. The application of this approach for image velocimetry requires a distinct thermal signal to

30 be present from either natural (e.g. tributary confluences with water of differing thermal properties), or artificial sources. In this instance, an artificial thermal signal was introduced in the form of ice dices. These were deployed upstream of the bridge and were observed transiting across the field of view as a result of their thermal properties being sufficiently different to that of the water surface. Despite the image resolution being a modest 318×197 pixels with a frame rate of 5Hz, this was still sufficient to enable movement of the ice-dices to be tracked. Geometric calibration of the images was achieved by identifying features

of known dimensions within the video sequence (i.e. three wooden sticks). The pixel dimensions of the processed imagery are 0.009m. Here we present an image sequence consisting of 80 consecutive frames captured over sixteen seconds. Validation data is available in the form of velocity measurements taken at just 3cm below the water surface at four locations along the stream cross-section using an OTT Hydromet C2 current meter (Tauro et al., 2017).

2.6 La Morge River, France

As part of Electricité De France's (EDF) network of monitoring stations for the optimal management of water resources, image-based velocimetry approaches have been deployed to supplement their existing network of over 300 hydrological monitoring stations. This approach has been specifically adopted with the aim of reducing uncertainty under high flow conditions (Hauet, 2016). These conditions can develop rapidly, particularly during the summer months as a result of convective storms, posing difficulties for traditional monitoring approaches. However, this setup may also be applied to capture images for the determination of surface velocity under more quiescent conditions. Here, we present images captured on 13th January 2015 in the small ($46\,\mathrm{km}^2$), urban catchment of La Morge with a mean altitude of $270\,\mathrm{m}$. Flow conditions were typical with a cross-section width of $7.2\,\mathrm{m}$, mean depth of $0.41\,\mathrm{m}$, and mean velocity of $0.39\ \mathrm{ms}^{-1}$. The imaging system used consisted of an analog Panasonic WV-CP500 camera with a focal length of $4\,\mathrm{mm}$. This camera was mounted at an elevated position on a $3\,\mathrm{m}$ pole on the right bank of the channel, oriented in an upstream direction. Images were collected with an effective pixel resolution of 640×480 at a frame rate of $5\,\mathrm{Hz}$ for a duration of $10\,\mathrm{s}$ resulting in the generation of 48 images. On this occasion, manual seeding of corn chips took place immediately upstream of the camera's field-of-view to enhance the occurrence of features for tracking purposes. This is typically required where natural seeding is inhomogeneous, or completely lacking, in some settings under low-flow conditions. Following acquisition of the footage, images were converted to grayscale, and orthorectified using Fudaa-LSPIV to generate images in which 1 pixel represents a real-world distance of $0.01\,\mathrm{m}$. Validation velocity data was acquired through the use of a mechanical current meter, with measurements taken at 0.2, 0.6, and 0.8 of the river depth. 15 measurements were made along the cross-section, at intervals of $0.5\,\mathrm{m}$.

2.7 St-Julien torrent, France

A high-magnitude flash flood event occurred in the St-Julien torrent system during August 2011. This was captured by a local storm chaser using a Canon EOS 5D mark II camera with a $16\,\mathrm{mm}$ fisheye Zenitar lens. Like many headwater systems across Europe, no hydrological monitoring networks are present in this torrent system. Therefore this footage provides a rare insight into the hydraulic processes occurring during a flash flood in a steep, small ($20\,\mathrm{km}^2$), torrent system. The footage itself was recorded at a resolution of 1920×1080px at a frame rate of $25\,\mathrm{Hz}$ (Figure 3a). The footage was not filmed from a fixed location therefore complications involving camera movement, and orthorectification had to be overcome. These steps are explained in detail in Le Boursicaud et al. (2016). Following correction for these factors, a sequence of 51 consecutive and geometrically stable images are produced (Figure 3b). Each pixel width represents a metric scale of $0.03\,\mathrm{m}$.

Figure 3. (a) Original footage of a flash flood in the St-Julien torrent acquired by a storm chaser equipped with Canon EOS 5D mark II camera. The direction of flow is from the top of the frame, moving towards the bottom of the image; (b) Orthorectified and geometrically stable image with the field of view clipped to the lower 50% of the image. The direction of flow is from the bottom of the frame, moving towards the top of the image.

2.8 River La Vence, France

On May 8th, 2019, a Samsung Galaxy S7 was utilised to capture footage for image velocimetry analysis on the River La Vence, a $63.75\,\mathrm{km^2}$ catchment in France. At the time of deployment, the river width was approximately $6.7\,\mathrm{m}$, the river stage was $0.44\,\mathrm{m}$, with an observed discharge of $1.15\,\mathrm{m^3\,s^{-1}}$. The camera was fixed in location with the camera lens at

5 an approximately $31°$ from the water surface and the image x-axis at approximately perpendicular to the direction of flow. Images were collected for a duration of 5 seconds at a resolution of 1920×1080px and frame rate of 30Hz. The presence of visible turbulent structures advecting downstream offer the potential for the extraction of surface velocity information from this footage. Image pre-processing consisted of orthorectification, and color conversion to gray-scale. 150 consecutive images which have been subjected to these processing steps are presented here at their original frame rate of 30Hz. The pixel

10 dimensions of the processed imagery are 0.008m in the x and y-axis. Validation data was recorded by means of a mobile ADCP (HydroProfiler M-pro).

2.9 River Tiber, Italy

A permanent gauge station on the River Tiber, Italy was installed to test the feasibility for automated image velocimetry methods to quantify the flow rates of a major European river with a catchment area of $17\,460\,\mathrm{km^2}$. This deployment involves

15 the use of a Mobotix FlexMount S15 IP camera attached to the underside of Ponte del Foro Italico, in the city of Rome (Tauro et al., 2016a). The wide angle lens on the SP15 camera introduces distortion into the images, which was subsequently removed using the Adobe Photoshop Lens correction filter. In a similar setup to the first of the River Brenta approaches, this camera is positioned orthogonal to the water surface, thereby circumventing the need for orthorectification of the generated images. Transformation of the camera pixels (px) to metric units (m) was again achieved by firing lasers of a known distance apart

20 at the water surface. The image can be scaled to metric distances given: 1px = $0.016\,\mathrm{m}$. The camera itself generated videos with a resolution of 2048×768px. However these were sub-sampled to 865×530px at a frame rate of ≈ 6.95Hz during pre-possessing. The data specifically presented here consists of 410 consecutive frames collected over a $60\,\mathrm{second}$ period during a moderate flood event in February 2015. At the time of acquisition, the river stage was $7.23\,\mathrm{m}$, and average surface velocity (measured by a RVM20 speed surface velocity radar) was $2.33\mathrm{ms^{-1}}$ (Tauro et al., 2017).

25 ## 2.10 River Bradano, Italy

On 14th October 2016, an experiment was undertaken in order to explore the optimal setup for the acquisition of surface flow velocity measurements using an UAS (Dal Sasso et al., 2018). The experiment took place in the valley portion of the Bradano River, located in the Basilicata region of Italy. This large alluvial river has a catchment area of $2581\,\mathrm{km^2}$ and is characterised by low gradient (0.1%) and low relative submergence (Dal Sasso et al., 2018). At the time of the experiment, the cross-section

30 width was $11.4\,\mathrm{m}$, with a maximum depth of $0.80\,\mathrm{m}$. The average surface velocity was $0.75\mathrm{ms^{-1}}$ and total discharge was $3.97\,\mathrm{m^3\,s^{-1}}$. During the experiment, a DJI Phantom 3 Pro UAS equipped with a Sony EXMOR 1/2.3" CMOS camera sensor was deployed.

This system hovered over the centre of the River Bradano with a nadir camera positioned perpendicular to the direction of flow. Flight altitude was set at $10\,\mathrm{m}$ in order to capture an area of $17.0 \times 9.6\mathrm{m}^2$, including the entire cross-section of interest (with a width of approximately $11.4\,\mathrm{m}$). Video footage was captured for a duration of $1\,\mathrm{min}\,43\,\mathrm{s}$ at a pixel resolution of 1920×1080, and a frame rate of $24\,\mathrm{Hz}$. Due to the high turbidity of the flow, there is a weak natural contrast across the

5   image which diminishes the number of naturally occurring, visible tracers. Therefore, throughout the duration of the footage, operatives manually introduced charcoal to the water surface immediately upstream of the monitoring site. The color of these particles was sufficiently distinct from the background to enable their displacement to be optically tracked. However, the distribution of these tracers is generally limited to the central portion of the flow which may limit the availability of traceable features towards the channel boundaries. Following collection of the footage, a number of processing steps were subsequently

10   undertaken. This included conversion of the grayscale images to black and white, and contrast correction in order to more prominently highlight the artificial tracers on the water surface. 600 images which have been subjected to these processing steps are available at their original resolution and frame rate. Transformation of the camera pixel units to metric distance can be achieved using the following function: $1\mathrm{px} = 0.009\,\mathrm{m}$. Validation data in the form of surface velocities were obtained at five points in the cross-section, at $1\,\mathrm{m}$ intervals using a Seba F1 current flow meter.

15   ## 2.11   River Noce, Italy

On 26th July 2017, in the middle reaches of the $413\,\mathrm{km}^2$, single-thread, River Noce, a DJI Phantom 3 Pro UAS Sony EXMOR 1/2.3" CMOS sensor was deployed to capture footage for image velocimetry analysis (Dal Sasso et al., 2018). At the time of deployment, water levels were low with an observed discharge of $1.70\,\mathrm{m}^3\,\mathrm{s}^{-1}$. Turbidity was also minimal resulting in the gravel bed being distinctly visible in the footage. The camera was oriented with its x-axis perpendicular to the water surface

20   enabling the $14.6\,\mathrm{m}$ wide channel to be fully observed (Figure 4a). Images were collected for a duration of $1\,\mathrm{min}\,48\,\mathrm{s}$ at a resolution of $3840 \times 2160\mathrm{px}$ and frame rate of $24\,\mathrm{Hz}$. The clear water and bright sunlight results in non-homogeneous illumination of the water surface. This is particularly apparent in the lower left quarter of the video frame. Naturally occurring tracers are also largely absent making these challenging conditions for the application of image velocimetry techniques. To offset these issues, wood chips were introduced upstream of the monitoring location. These features were visibly brighter than the

25   background enabling their transition to be detected optically. Image processing consisted of contrast stretching and conversion of grayscale images to black and white in order to enhance the visibility of the artificial tracers against the background (Figure 4b). 70 consecutive images which have been subjected to these processing steps are presented here at a downscaled resolution of $1920 \times 1080\mathrm{px}$ and frame rate of $12\,\mathrm{Hz}$. Following sub-sampling, each pixel in the image represents a distance of $0.009\,\mathrm{m}$ in metric units. Validation data in the form of surface velocities were obtained at ten locations, at $1\,\mathrm{m}$ intervals, along the

30   cross-section using a Seba F1 current flow meter.

2.12   River Karehalla, India

On 19th June 2018, a Vivotek IB836BA-HT network surveillance camera was utilised to capture footage for image velocimetry analysis on the River Karehalla in India ($12.835°\mathrm{N}$, $75.716°\mathrm{E}$). At the time of deployment, the channel width was approx-
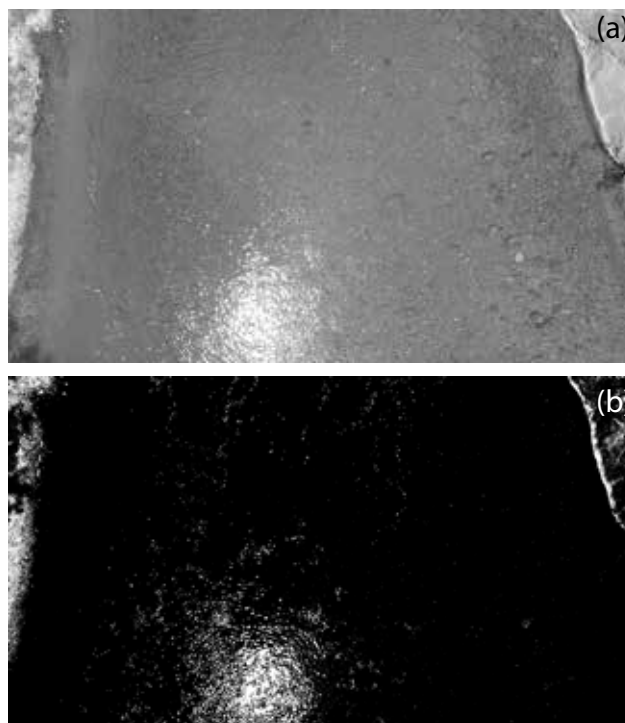
Figure 4. (a) Grayscale footage acquired by the Phantom 3 UAS over the River Noce, and (b) following contrast stretching.

imately $8.36\,\mathrm{m}$, the river stage was $0.606\,\mathrm{m}$, with an observed discharge of $3.003\,\mathrm{m}^3\,\mathrm{s}^{-1}$. The camera was fixed in location with the camera lens at an approximately $30°$ from nadir and the image x-axis at approximately $5°$ from perpendicular to the direction of flow. Images were collected for a duration of $4.6\,\mathrm{s}$ at a resolution of $1920{\times}1080\mathrm{px}$ and frame rate of $30\,\mathrm{Hz}$. Highly visible, naturally occurring, turbulent structures that are advecting downstream offer the potential for the extraction of surface

5 velocity information from these images. Image pre-processing consisted of orthorectification, and color conversion to grayscale. 144 consecutive images which have been subjected to these processing steps are presented here at their original frame rate of $30\,\mathrm{Hz}$. The pixel dimensions of the processed imagery is $0.01\,\mathrm{m}$ in the x and y-axis. Validation data was acquired by means of a HydroProfiler M-pro ADCP.

3 Conclusions

10 Applied hydrology research, focussing on the quantification of fluid flow processes in river systems, has been greatly enhanced by the availability of large-scale image velocimetry techniques (e.g. Table A1). The flexibility of these approaches has led to improvements in the understanding of hydrological processes in otherwise difficult to access environments. This has been possible through image capture using a range of platforms including: unmanned aerial systems, thermal infra-red cameras, Go-Pro's, and IP cameras, which enable non-contact sensing of the waterbody. Consequently, a growing, but disparate, range

of imagery datasets have been produced (e.g. Table A2). Here we collate and describe a range of these example datasets, most of which have validation data in the form of velocity measurements undertaken using standard operational approaches (e.g. current flow meter, ADCP, radar). This unique dataset offers the hydrological community the opportunity to conduct image velocimetry benchmarking studies in order to assess the accuracy of existing approaches under a range of differing conditions.

5 The generation of similar standardised sets of images are widely used to evaluate the effectiveness and accuracy of algorithms in related fields such as fluid mechanics (e.g. Okamoto et al., 2000), and we envisage such a dataset for large-scale fluvial environments will encourage further scientific assessment and development of image velocimetry approaches. Ultimately, forensic assessment of these techniques will provide researchers and competent authorities with a greater understanding of their applicability and limitations.

10 ## 4 Data availability

Datasets presented in this manuscript can be readily downloaded from the following website: https://data.4tu.nl/repository/uuid:
34764be1-31f9-4626-8b11-705b4f66b95a. Validation data is available for 12 of the 13 case studies presented. Please contact the corresponding author for details (Perks et al., 2019).

Table A1. Details of software developed for image velocimetry analysis

Software	Key Functions	Availability
Fudaa-LSPIV[a]	Sample images from movies, image orthorectification, cross-correlation, data filtering, discharge computation	Open source interface, free executables
KLT-IV[b]	Lens distortion removal, image orthorectification, tracking individual trajectories	Proprietary software
KU-STIV[c]	Distortion removal, orthorectification, image stabilisation, image pattern coherence	Proprietary software
LSPIV app[d]	Camera calibration, image orthorectification, cross-correlation, image pattern coherence	Free app for Android and iOS
MAT PIV[e]	Image coordinate transformation, cross-correlation, post-processing filters	Free toolbox for MATLAB
OTV[f]	Tracking individual trajectories and average surface flow velocity estimation	Proprietary software
Photrack. SSIV[g]	Image orthorectification, cross-correlation, flow surface structure filtering, results filtering, discharge estimation. Stand-alone camera system for continuous measurement (DischargeKeeper), or in a smart-phone application (DischargeApp)	Proprietary software
PIVlab[h]	Image pre-processing, direct cross-correlation, discrete Fourier transform, sub-pixel solutiona, post-processing tools	Free toolbox for MATLAB
PTVlab[i]	Image pre-processing, cross-correlation, relaxation algorithm, dynamic threshold binarization, iterative relaxation, tracking of individual trajectories, post-processing tools	Free toolbox for MATLAB
PTV-Stream[j]	Tracking individual trajectories and average surface flow velocity estimation	Proprietary software
RIVeR[k]	Image extraction from video, image processing (PIVlab or PTVlab), rectification of velocities to real-world units, discharge calculation	Free toolbox for MATLAB

[a]Le Coz et al. (2014); [b]Perks et al. (2016); [c]Fujita et al. (2007); [d]Tsubaki (2018); [e]Sveen and Cowen (2004); [f]Tauro et al. (2018b); [g]Leitão et al. (2018); [h]Thielicke and Stamhuis (2014); [i]Brevis et al. (2011); [j]Tauro et al. (2019); [k]Patalano et al. (2017)

Table A2. Experimental setup during data acquisition, details of subsequent image pre-processing, availability of validation data and published analysis.

Identifier	Data Acquisition	Pre-processing	Validation Data	Image Velocimetry Software Used	Published Analysis
River Arrow (a)	DJI Phantom Pro 4 UAS	Conversion to grayscale intensity Orthorectification Image sequence sub-sampled	Yes	Fudaa-LSPIV	N/A
River Arrow (b)	Go Pro Hero 4	Conversion to grayscale intensity Orthorectification Image sequence sub-sampled	Yes	Fudaa-LSPIV	N/A
River Dart	Hikvision EXIR	Distortion removal Orthorectification	Yes	KLT-IV	N/A
River Thalhofen	Vivotek IB836BA-HT	Orthorectification Conversion to grayscale intensity	Yes	Photrack. SSIV	N/A
Murg River	DJI Phantom FC40 UAS with GoPro Hero3+	Orthorectification	Yes	PIVlab	Detert et al. (2017)
River Brenta (a)	GoPro Hero 4	Distortion removal Gamma correction	Yes	PIVlab & PTVlab	Tauro et al. (2017)
River Brenta (b)	FLIR SC500	Orthorectification Extraction of RGB from thermal	Yes	PTVlab	Tauro and Grimaldi (2017)
La Morge	WV-CP500	Orthorectification	Yes	Fudaa-LSPIV	Hauet (2016)

Identifier	Data Acquisition	Pre-processing	Validation Data	Image Velocimetry Software Used	Published Analysis
St-Julien torrent	Canon EOS 5D	Distortion removal Orthorectification Image stabilisation	No	Fudaa-LSPIV	Le Boursicaud et al. (2016)
River La Vence	Samsung Galaxy S7	Orthorectification Conversion to grayscale intensity	Yes	Photrack. SSIV	N/A
River Tiber	Mobotix S15	Distortion removal Conversion to grayscale intensity	Yes	PIVlab & PTVlab	Tauro et al. (2017)
River Bradano	DJI Phantom 3 Pro UAS with Sony 1/2.3" CMOS sensor	Conversion to black and white images Contrast correction	Yes	PTVlab	Dal Sasso et al. (2018)
River Noce	DJI Phantom 3 Pro UAS with Sony 1/2.3" CMOS sensor	Contrast stretching Conversion to black and white images Image sequence sub-sampled	Yes	PTVlab	Dal Sasso et al. (2018)
River Karehalla	Vivotek IB836BA-HT	Orthorectification Conversion to grayscale intensity	Yes	Photrack. SSIV	N/A

Author contributions. This article and dataset compilation was initially proposed by SM and SG. MP led the production of the manuscript. Each co-author contributed to the writing, and the contribution of datasets.

Competing interests. The authors declare that they have no conflict of interest.

Acknowledgements. This work was funded by the COST Action CA16219 "HARMONIOUS—Harmonization of UAS techniques for agri-
5 cultural and natural ecosystems monitoring". MP and BH acknowledge additional funding from NERC grant NE/K008781/1 "Suscep-
tibility of catchments to INTense RAinfall and flooding (SINATRA)", and the Environment Agency. SG and FT acknowledge support
by Ministero degli Affari Esteri project 2015 Italy-USA PGR00175 and by POR-FESR 2014-2020 n. 737616 INFRASAFE. The con-
tribution of the Murg River dataset was kindly made available by Dr Martin Detert. The Murg River dataset can also be accessed at:
https://figshare.com/articles/S1S2S3_Murg_20160406_zip/4680715/1.

References

Adrian, R. J.: Scattering particle characteristics and their effect on pulsed laser measurements of fluid flow: speckle velocimetry vs particle image velocimetry, Appl. Opt., 23, 1690–1691, https://doi.org/10.1364/AO.23.001690, 1984.

Agisoft: Agisoft PhotoScan Professional Edition (version 1.1.6), https://www.agisoft.com.

5 Brevis, W., Niño, Y., and H. Jirka, G.: Integrating cross-correlation and relaxation algorithms for particle tracking velocimetry, Experiments in Fluids, 50, 135–147, 2011.

Dal Sasso, S. F., Pizarro, A., Samela, C., Mita, L., and Manfreda, S.: Exploring the optimal experimental setup for surface flow velocity measurements using PTV, Environmental Monitoring and Assessment, 190, 460, https://doi.org/10.1007/s10661-018-6848-3, 2018.

Detert, M. and Weitbrecht, V.: A low-cost airborne velocimetry system: proof of concept, Journal of Hydraulic Research, 53, 532–539,
10 https://doi.org/10.1080/00221686.2015.1054322, 2015.

Detert, M., Johnson, E. D., and Weitbrecht, V.: Proof-of-concept for low-cost and noncontact synoptic airborne river flow measurements, International Journal of Remote Sensing, 38, 2780–2807, https://doi.org/10.1080/01431161.2017.1294782, 2017.

Dudderar, T. D. and Simpkins, P. G.: Laser speckle photography in a fluid medium, Nature, 270, http://dx.doi.org/10.1038/270045a0, 1977.

Fujita, I., Muste, M., and Kruger, A.: Large-scale particle image velocimetry for flow analysis in hydraulic engineering applications, Journal
15 of Hydraulic Research, 36, 397–414, https://doi.org/10.1080/00221689809498626, 1998.

Fujita, I., Watanabe, H., and Tsubaki, R.: Development of a non-intrusive and efficient flow monitoring technique: The space-time image velocimetry (STIV), International Journal of River Basin Management, 5, 105–114, https://doi.org/10.1080/15715124.2007.9635310, 2007.

Harpold, A., Mostaghimi, S., Vlachos, P. P., Brannan, K., and Dillaha, T.: Stream discharge measurement using a large-scale particle image
20 velocimetry (LSPIV) prototype, Transactions of the ASABE, 49, 1791–1805, 2006.

Hauet, A.: Monitoring river flood using fixed image-based stations: Experience feedback from 3 rivers in France, in: River Flow 2016: Iowa City, USA, July 11-14, 2016, edited by Constantinescu, G., Garcia, M., and Hanes, D., pp. 541–547, CRC Press, Boca Raton, USA, https://books.google.co.uk/books?id=blOzDAAAQBAJ, 2016.

ISO 24578:2012: Hydrometry — Acoustic Doppler profiler — Method and application for measurement of flow in open channels, Standard,
25 International Organization for Standardization, Geneva, CH, 2012.

Le Boursicaud, R., Pénard, L., Hauet, A., Thollet, F., and Le Coz, J.: Gauging extreme floods on YouTube: application of LSPIV to home movies for the post-event determination of stream discharges, Hydrological Processes, 30, 90–105, https://doi.org/10.1002/hyp.10532, 2016.

Le Coz, J., Jodeau, M., Hauet, A., Marchand, B., and Le Boursicaud, R.: Image-based velocity and discharge measurements in field and
30 laboratory river engineering studies using the free FUDAA-LSPIV software, Proceedings of the International Conference on Fluvial Hydraulics, River Flow 2014, pp. 1961–1967, 2014.

Leitão, J. P., Peña-Haro, S., Lüthi, B., Scheidegger, A., and de Vitry, M. M.: Urban overland runoff velocity measurement with consumer-grade surveillance cameras and surface structure image velocimetry, Journal of Hydrology, 565, 791 – 804, https://doi.org/https://doi.org/10.1016/j.jhydrol.2018.09.001, http://www.sciencedirect.com/science/article/pii/S0022169418306875,
35 2018.

Mishra, A. K. and Coulibaly, P.: Developments in hydrometric network design: A review, Reviews of Geophysics, 47, https://doi.org/10.1029/2007RG000243, https://agupubs.onlinelibrary.wiley.com/doi/abs/10.1029/2007RG000243, 2009.

Okamoto, K., Nishio, S., Saga, T., and Kobayashi, T.: Standard images for particle-image velocimetry, Measurement Science and Technology, 11, 685–691, https://doi.org/10.1088/0957-0233/11/6/311, https://doi.org/10.1088%2F0957-0233%2F11%2F6%2F311, 2000.

Patalano, A., García, C. M., and Rodríguez, A.: Rectification of Image Velocity Results (RIVeR): A simple and user-friendly toolbox for large scale water surface Particle Image Velocimetry (PIV) and Particle Tracking Velocimetry (PTV), Computers & Geosciences, 109, 323 – 330, https://doi.org/https://doi.org/10.1016/j.cageo.2017.07.009, http://www.sciencedirect.com/science/article/pii/S0098300417307045, 2017.

Perks, M. T., Russell, A. J., and Large, A. R. G.: Technical Note: Advances in flash flood monitoring using unmanned aerial vehicles (UAVs), Hydrology and Earth System Sciences, 20, 4005–4015, https://doi.org/10.5194/hess-20-4005-2016, 2016.

Perks, M. T., Dal Sasso, S., Detert, M., Hauet, A., Pearce, S., Peña-Haro, S., Tauro, F., Grimaldi, S., Hortobágyi, B., Jodeau, M., Le Coz, J., Maddock, I., Pénard, L., and Manfreda, S.: Data on the harmonization of image velocimetry techniques, from six different countries, https://doi.org/10.4121/UUID:34764BE1-31F9-4626-8B11-705B4F66B95A, https://data.4tu.nl/repository/uuid: 34764be1-31f9-4626-8b11-705b4f66b95a, 2019.

Pickering, C. J. D. and Halliwell, N. A.: Laser speckle photography and particle image velocimetry: photographic film noise, Appl. Opt., 23, 2961–2969, https://doi.org/10.1364/AO.23.002961, 1984.

Sveen, J. K. and Cowen, E. A.: Quantitative imaging techniques and their application to wavy flows, pp. 1–49, https://doi.org/10.1142/9789812796615_0001, 2004.

Tauro, F. and Grimaldi, S.: Ice dices for monitoring stream surface velocity, Journal of Hydro-environment Research, 14, 143 – 149, https://doi.org/https://doi.org/10.1016/j.jher.2016.09.001, 2017.

Tauro, F., Porfiri, M., and Grimaldi, S.: Orienting the camera and firing lasers to enhance large scale particle image velocimetry for streamflow monitoring, Water Resources Research, 50, 7470–7483, https://doi.org/10.1002/2014WR015952, 2014.

Tauro, F., Petroselli, A., Porfiri, M., Giandomenico, L., Bernardi, G., Mele, F., Spina, D., and Grimaldi, S.: A novel permanent gauge-cam station for surface-flow observations on the Tiber River, Geoscientific Instrumentation, Methods and Data Systems, 5, 241–251, https://doi.org/10.5194/gi-5-241-2016, 2016a.

Tauro, F., Porfiri, M., and Grimaldi, S.: Surface flow measurements from drones, Journal of Hydrology, 540, 240 – 245, https://doi.org/https://doi.org/10.1016/j.jhydrol.2016.06.012, 2016b.

Tauro, F., Piscopia, R., and Grimaldi, S.: Streamflow Observations From Cameras: Large-Scale Particle Image Velocimetry or Particle Tracking Velocimetry?, Water Resources Research, 53, 10 374–10 394, https://doi.org/10.1002/2017WR020848, 2017.

Tauro, F., Selker, J., van de Giesen, N., Abrate, T., Uijlenhoet, R., Porfiri, M., Manfreda, S., Caylor, K., Moramarco, T., Benveniste, J., Ciraolo, G., Estes, L., Domeneghetti, A., Perks, M. T., Corbari, C., Rabiei, E., Ravazzani, G., Bogena, H., Harfouche, A., Brocca, L., Maltese, A., Wickert, A., Tarpanelli, A., Good, S., Alcala, J. M. L., Petroselli, A., Cudennec, C., Blume, T., Hut, R., and Grimaldi, S.: Measurements and Observations in the XXI century (MOXXI): innovation and multi-disciplinarity to sense the hydrological cycle, Hydrological Sciences Journal, 63, 169–196, https://doi.org/10.1080/02626667.2017.1420191, 2018a.

Tauro, F., Tosi, F., Mattoccia, S., Toth, E., Piscopia, R., and Grimaldi, S.: Optical Tracking Velocimetry (OTV): Leveraging Optical Flow and Trajectory-Based Filtering for Surface Streamflow Observations, Remote Sensing, 10, https://doi.org/10.3390/rs10122010, https://www.mdpi.com/2072-4292/10/12/2010, 2018b.

Tauro, F., Piscopia, R., and Grimaldi, S.: PTV-Stream: A simplified particle tracking velocimetry framework for stream surface flow monitoring, CATENA, 172, 378 – 386, https://doi.org/https://doi.org/10.1016/j.catena.2018.09.009, http://www.sciencedirect.com/science/article/pii/S0341816218303771, 2019.

Thielicke, W. and Stamhuis, E.: PIVlab – Towards User-friendly, Affordable and Accurate Digital Particle Image Velocimetry in MATLAB, Journal of Open Research Software, 2, e30, http://doi.org/10.5334/jors.bl, 2014.

Tsubaki, R.: LSPIV app, https://sites.google.com/site/rtsubaki/lspiv-app, 2018.